
JOURNAL OF THE AMERICAN CHEMICAL SOCIETY

Mapping the Potential Energy Surfaces of the 1,6-Diphenyl-1,3,5-hexatriene Ground and Triplet States

Jack Saltiel,* Janell M. Crowder, and Shujun Wang

Contribution from the Department of Chemistry, The Florida State University,
Tallahassee, Florida 32306-4390

Received July 20, 1998

Abstract: The relative energies of the ground state isomers of 1,6-diphenyl-1,3,5-hexatriene (DPH) in benzene are determined from the temperature dependence of the equilibrium isomer composition obtained with the use of diphenyl diselenide as isomerization catalyst. In the triplet state, DPH exists as an equilibrium mixture of all-trans (ttt), trans,cis,trans (tct), cis,trans,trans (ctt), and cis,cis,trans (cct) isomers. Under degassed conditions, photoisomerization of the triplets is primarily bimolecular, involving a quantum chain process. Oxygen eliminates the quantum chain process by efficient deactivation of DPH triplets thereby revealing the triplet state isomeric composition. The temperature dependencies of the fluorenone-sensitized photoisomerization quantum yields and photostationary states for DPH in air-saturated benzene provide two independent measures of the temperature dependence of the equilibrium contribution of the isomeric triplets. They reveal the relative energies of the DPH triplet isomers. Together with the known 34 kcal/mol triplet energy of *ttt*-DPH, these results define points on the potential energy surfaces of the ground and triplet states corresponding to the equilibrium geometries of the four observed DPH isomers. At these geometries the two surfaces roughly parallel each other. Complete equilibration of isomeric triplets within 100 ns requires that the energies of triplet biradical transition states be no higher than 40.3 kcal/mol. Estimated radical stabilization energies give 40.2 and 41.6 kcal/mol for the energies of biradical transition states for central and terminal bond isomerization, respectively, in the ground state of *ttt*-DPH.

Introduction

The photophysical and photochemical events that follow excitation of a molecule to its lowest electronically excited triplet state are controlled, in large measure, by the shapes and proximity of the potential energy surfaces of the ground and triplet states. Unimolecular photoisomerizations occur through geometry changes of the initially excited molecule that move it along minimum energy paths to energy minima on the excited-state surface from which intersystem crossing to the ground state may access geometries favorable to product formation. The cis \rightleftharpoons trans photoisomerizations of triplet olefins provide excellent illustrations of such events. Two limiting cases have been identified. The first is exemplified by the stilbenes for which a

common relaxed triplet is accessed from both isomers by torsional displacement about the central bond to a perpendicular geometry, $^3p^*$. Decay from $^3p^*$ leads to partitioning of the triplets between the two ground-state isomers.¹ The second case is exemplified by the 1-(2-anthryl)-2-phenylethenes (APEs).² Here cis \rightarrow trans photoisomerization in the triplet state occurs as an adiabatic one-way process, $^3c^* \rightarrow ^3t^*$, with $^3p^*$ an energy

(1) For reviews see: (a) Saltiel, J.; D'Agostino, J.; Megarity, E. D.; Metts, L.; Neuberger, K. R.; Wrighton, M.; Zafriou, O. C. *Org. Photochem.* **1973**, *3*, 1–113. (b) Saltiel, J.; Charlton, J. L. *Rearrangements in Ground and Excited States*; de Mayo, P., Ed.; Academic Press: New York, 1980; Vol. 3, pp 25–89. (c) Görner, H.; Kuhn, H. J. *Adv. Photochem.* **1995**, *19*, 1–118.

(2) For reviews see: (a) Arai, T.; Tokumaru, K. *Chem. Rev.* **1993**, *93*, 23–39. (b) Tokumaru, K.; Arai, T. *Bull. Chem. Soc. Jpn.* **1995**, *68*, 1065–1087.

maximum corresponding to the transition state for the reaction. Unimolecular radiationless decay from $^3t^*$ or triplet excitation transfer from $^3t^*$ to *cis*-APE (the first step of a quantum chain process) completes the *cis* \rightarrow *trans* photoreaction.

In fluid solutions DPH triplets exist as an equilibrium mixture of all-*trans* (ttt) *trans,cis,trans* (tct), *cis,trans,trans* (ctt) and, in trace amount, *cis,cis,trans* (cct) isomers.³ Excitation of any one of the DPH isomers to the triplet state rapidly gives a common equilibrium mixture of triplet isomers whose decay leads to product isomer formation. Thus, the initial isomerization occurs adiabatically in the triplet state as in APE, but since, in this case, it is reversible, it occurs in more than one direction as in the stilbenes.

This paper reports the temperature dependencies of DPH isomer compositions in the ground and triplet states. The resulting ΔH 's between the DPH isomers in these states provide anchor points for the construction of the respective potential energy surfaces that control the photochemical behavior of this system.

Experimental Section

Materials. Diphenyl diselenide (Aldrich, 98%) was used as received. The sources and purification methods of the other materials were given previously.³

Analytical Procedures. These were as previously described,³ except that samples containing diphenyl diselenide were first passed through a small column of silver nitrate coated alumina with the aid of 20 mL of benzene eluent. This procedure retains all the diphenyl diselenide on the column while allowing all DPH to pass without altering the isomeric distribution. The step was essential because diphenyl diselenide interferes with the HPLC analysis of the DPH isomers. Prior to the HPLC analysis anthracene was added as internal standard.³ The benzene was removed under reduced pressure and the residue was diluted to approximately 3 mL with Fisher Optima hexane, which was also used as eluent for the HPLC analyses.³ Analyses of successively diluted samples assured selection of conditions of linear response of the HPLC detection system. Even at the lowest concentrations employed some saturation of the *ttt*-DPH signals is suspected. Sample preparation and handling were performed under nearly complete darkness to avoid unintentional isomerization.

Irradiation Procedures. Irradiation procedures were as previously described³ except that the Osram HBO 200-W super high-pressure mercury lamp was used in all experiments. A high-intensity Bausch and Lomb monochromator was used to excite samples at 425 nm for both diphenyl diselenide catalyzed (degassed benzene solutions, thermal) and fluorenone-sensitized (air-saturated benzene solutions, triplet) stationary state determinations. For quantum yield measurements in the presence of air, excitation of the fluorenone sensitizer was at 435 nm. The rotating miniature merry-go-round was employed for these measurements and samples were flame sealed at a constriction in the presence of air. The sealing prevents any loss of solvent at the higher temperatures but introduces some reduction and uncertainty in the oxygen concentration. The aluminum merry-go-round and samples were immersed in water in a dewar. Temperature control was provided by a Neslab RTE-4DD refrigerated circulating bath connected to a copper coil positioned about the merry-go-around in the dewar. Temperatures were monitored by use of an Omega Engineering Model 199P2 RTD digital thermometer equipped with a calibrated probe.

Absorption Spectra. Absorption spectra were measured with the use of a Perkin-Elmer Lambda-5 spectrophotometer interfaced with a Dell Corp. 12 MHz 80286/87 microcomputer.

Results

Thermal Equilibrations. In initial experiments iodine (2.30×10^{-4} M in benzene or 2.21×10^{-4} M in *tert*-butylbenzene)

Table 1. DPH Isomer Compositions at Thermal Equilibrium^a

<i>T</i> , °C	$10^2 f_{\text{ttt}}^b$	$10^2 f_{\text{tct}}$	$10^2 f_{\text{ctt}}$	$10^2 f_{\text{cct}}$
9.8	92.7	5.9 ₁	1.32	0.12 ₉
18.1	91.9	6.3 ₄	1.64	0.13 ₁
27.3	91.6	6.5 ₆	1.71	0.16 ₉
36.8	90.9	6.9 ₉	1.89	0.20 ₉
47.2	90.7	7.1 ₃	1.89	0.25 ₁
58.0	88.9	8.5 ₃	2.26	0.28 ₂
69.7	87.8	8.9 ₈	2.81	0.42 ₂

^a Estimated uncertainties are ± 0.2 °C for *T* and $\pm 3\%$ for the HPLC analyses of *tct*- and *ctt*-DPH; a larger uncertainty ($\pm 20\%$) is expected for *cct*-DPH (see text). ^b Calculated from $f_{\text{ttt}} = 1 - (f_{\text{tct}} + f_{\text{ctt}} + f_{\text{cct}})$.

was thermally or photochemically ($\lambda = 530$ nm) dissociated to yield iodine atoms as catalysts for the isomerization of *ttt*-DPH (1.08×10^{-3} M). Degassed and air-saturated 3 mL samples were equilibrated at temperatures ranging from -10 to 160 °C. At temperatures ≥ 100 °C erratic and irreproducible isomer distributions were obtained and large losses of DPH were observed, especially in the presence of air. Use of 250 nm as the monitoring wavelength, instead of the normally employed 350 nm monitoring wavelength,³ revealed the formation of a major and several minor side products. These products were not observed in the absence of iodine. The yield of the major product increases dramatically as the temperature is raised above 100 °C and is larger in the presence of air. Its identity was not pursued and this equilibration approach was abandoned. Further measurements were carried out on a benzene solution containing 5.1×10^{-4} M *ttt*-DPH and 5.0×10^{-3} M diphenyl diselenide. Equilibrium mixtures were obtained by irradiating degassed 3 mL samples for 2 h at each temperature. HPLC analyses, with anthracene as the internal standard, revealed no side products and established that, within $\pm 1\%$, DPH isomers accounted for all of the DPH present prior to equilibration at the two lowest (9.8 and 18.1 °C) and the two highest (58.0 and 69.7 °C) temperatures employed. Only 92% of the total DPH concentration was accounted for in both initial and final solutions, probably due to *ttt*-DPH signal saturation. Inability of the HPLC conditions to give baseline separation between *ctt*- and *cct*-DPH introduces some uncertainty in the derived concentrations of the latter, which is formed only in trace amounts. The area registered for *cct*-DPH by the HPLC integrator was found to be 10–25% lower than the area estimated by cutting and weighing 6 enlarged Xerox copies of the HPLC trace. The higher values were employed in the analysis. Equilibrium DPH isomer compositions are reported in Table 1.

Photostationary States. Three milliliter aliquots of an air-saturated benzene solution containing 3.93×10^{-3} M *ttt*-DPH and 0.024 M fluorenone were pipetted into Pyrex test tubes, 13 mm o.d., fitted with Teflon tape covered rubber stoppers. Control experiments established that irradiation of the stationary sample at 425 nm for 4 h was sufficient to attain the photostationary state at 10 °C, the lowest temperature used in our experiments. Each sample was irradiated for 4 h at each temperature and the experiment was repeated with a duplicate sample set. Analyses were as reported above. Decomposition of the *ctt*/*cct* combined peaks was achieved by assuming that the tail of the *ctt* peak is identical to the tail of the *tct* peak. The *cct* content was too small for the cutting and weighing procedure to be applied to the 10.8 and 10.9 °C samples. Photostationary state DPH isomer compositions are listed in Table 2.

Quantum Yields. The fluorenone-sensitized photoisomerization of *trans*-stilbene in benzene ($\phi_{t \rightarrow c} = 0.47^4$) was employed for actinometry. The actinometer's quantum yield reflects its

(3) Saltiel, J.; Wang, S.; Ko, D.-H.; Gormin, D. A. *J. Phys. Chem. A* 1998, 102, 5383–5392.

Table 2. Photostationary State Fractions for the Fluorenone-Sensitized Isomerization of DPH^a

<i>T</i> , °C	10 ² <i>f</i> _{ttt}	10 ² <i>f</i> _{tct}	10 ² <i>f</i> _{ctt}	10 ² <i>f</i> _{cct}
10.8	94.8	4.06	1.09	<i>b</i>
10.9 ^c	94.7	4.16	1.11	<i>b</i>
11.0	95.3	3.69	0.93 ₀	0.040 ₅
11.3	95.2	3.82	0.97 ₄	0.039 ₀
17.1	94.8	4.05	1.12	0.045 ₅
17.2	94.8	4.01	1.12	0.039 ₂
29.2	94.2	4.40	1.35	0.060 ₃
29.2	94.2	4.38	1.39	0.074 ₅
37.3	93.5	4.73	1.65	0.086 ₅
37.2	93.5	4.78	1.62	0.076 ₃
47.2	93.2	4.97	1.75	0.111
47.1	93.3	4.89	1.73	0.103
58.6	92.6	5.24	1.99	0.151
58.7	92.8	5.09	1.93	0.118
69.3	91.9	5.65	2.22	0.194

^a See footnotes *a* and *b* in Table 1. ^b Too small for accurate analysis. ^c This sample was irradiated for 8 h; two identical samples irradiated for 4 and 5 h gave *f*_{tct} values of 0.0407 and 0.0408, respectively.

Table 3. Quantum Yields for the Fluorenone-Sensitized Photoisomerization of *t**t**t*-DPH in Air-Saturated Benzene

<i>T</i> , °C	10 ⁴ [<i>t</i> <i>t</i> <i>t</i>], ^a M	10 ² ϕ _{ctt}	10 ² ϕ _{tct}	ϕ _{ctt} /ϕ _{tct}
8.7	2.7 ₈	0.26 ₇	1.2 ₀	0.219
	3.7 ₅	0.31 ₃	1.5 ₀	0.208
	5.5 ₆	0.40 ₅	1.9 ₁	0.213
	8.3 ₂	0.47 ₄	2.2 ₃	0.213
	11.1	0.55 ₁	2.5 ₄	0.217
20.0	13.9	0.69 ₅	3.0 ₄	0.229
	2.7 ₄	0.28 ₆	1.3 ₂	0.217
	3.7 ₀	0.37 ₃	1.7 ₂	0.217
	5.4 ₈	0.44 ₉	2.0 ₅	0.219
	8.2 ₁	0.55 ₉	2.5 ₂	0.222
32.2	11.0	0.65 ₀	2.9 ₈	0.218
	13.7	0.70 ₁	3.0 ₇	0.228
	2.7 ₀	0.55 ₃	2.1 ₁	0.262
	3.6 ₄	0.64 ₉	2.5 ₂	0.257
	5.4 ₀	0.74 ₈	2.9 ₇	0.252
45.5	8.0 ₉	0.80 ₅	3.1 ₃	0.257
	10.8	1.1 ₆	4.3 ₇	0.266
	13.5	1.1 ₁	4.3 ₂	0.256
	2.6 ₅	0.66 ₂	2.4 ₃	0.272
	3.5 ₈	0.83 ₇	2.9 ₈	0.281
60.0	5.3 ₁	0.89 ₂	3.2 ₈	0.272
	7.9 ₅	1.1 ₀	4.0 ₃	0.272
	10.6	1.3 ₆	4.8 ₄	0.280
	13.3	1.3 ₃	4.7 ₀	0.283
	2.6 ₁	0.75 ₃	2.5 ₀	0.301
	3.5 ₂	0.89 ₁	2.9 ₇	0.300
	5.2 ₁	1.1 ₁	3.6 ₁	0.306
	7.8 ₁	1.3 ₂	4.3 ₃	0.304
	10.4	1.6 ₃	5.2 ₄	0.310
	13.0	1.8 ₁	5.3 ₃	0.340

^a Concentrations were corrected for the temperature dependence of the density of benzene: $d(t) = 0.90034 - 0.001074t$, where t is in °C.⁶

intersystem crossing yield, $\phi_{is} = 0.93$,⁵ and a lower than unity (0.92) efficiency of the excitation transfer step.⁴ Since fluorenone is also the sensitizer for the photoisomerization of *t**t**t*-DPH, any change in ϕ_{is} with temperature cancels. However, the quantum yields listed in Table 3 are based on the assumptions that excitation transfer efficiency to *t**t**t*-DPH is completely efficient and that the efficiency of the excitation transfer step to *trans*-stilbene is temperature independent. Irradiation times were

(4) (a) Caldwell, R. A.; Gajewski, R. P. *J. Am. Chem. Soc.* **1971**, *93*, 532–534. (b) Valentine, D., Jr.; Hammond, G. S. *J. Am. Chem. Soc.* **1972**, *94*, 3449–3454.

(5) Lamola, A. A.; Hammond, G. S. *J. Chem. Phys.* **1965**, *43*, 2129–2135.

chosen so that conversions to the *cis* isomers were small, ensuring that back-reaction corrections,⁵ based on interpolated photostationary fractions from Table 2, did not significantly affect the results ($\leq 2\%$).

Discussion

The Ground State. Equilibration of the DPH isomers was reported first by Lunde and Zechmeister.⁷ On the basis of UV spectra it was shown that daylight lamp irradiation through Pyrex of air-saturated hexane solutions of the pure *t**t**t*, *t**c**t*, *c**t**t*, and *c**c**t* isomers in the presence of iodine gives identical isomer mixtures dominated by the *t**t**t* isomer. Chromatographic separation of the mixture obtained starting from *t**t**t*-DPH gave 93.9% *t**t**t*, 3.8% *c**t**t*, and 1.8% *t**c**t*.⁷ Exposure of the DPH isomers to light under these conditions probably interfered with the goal of establishing purely thermal equilibrium mixtures. In our experiments iodine was excited selectively and the resulting mixtures were consistently richer in the *t**c**t* than in the *c**t**t* isomer. However, in contrast to our observations on the iodine-catalyzed isomerization of the stilbenes,^{8,9} DPH isomer distributions were irreproducible and side reactions were dominant for $T \geq 100$ °C.

Diphenyl diselenide was first used by Alfimov and co-workers as an efficient catalyst for the equilibration of the stilbenes and other olefins.¹⁰ Isomerization is promoted by reversible addition of phenylselenium radicals to the double bond and regeneration of the catalyst by coupling of phenylselenium radicals is the only competing reaction. Lewis and co-workers have reported successful use of this catalyst,¹¹ and we had shown it to cleanly isomerize the 1,4-diphenyl-1,3-butadiene isomers.¹² The diphenyl diselenide catalyzed equilibration of the DPH isomers proceeds smoothly and cleanly. The equilibrium constants for



are ratios of the fractions given in Table 1, e.g., $K_{ctt} = f_{ctt}/f_{ttt}$. Plots of the data according to

$$\ln K = -\frac{\Delta H}{RT} + \frac{\Delta S}{R} \quad (4)$$

are shown in Figure 1 and give the ΔH and ΔS values in Table 4. Within experimental uncertainty the $\Delta H_{ctt} + \Delta H_{tct}$ sum equals ΔH_{cct} . The well-resolved vibronic structure of the spectrum of *t**c**t*-DPH⁷ suggests that the equilibrium geometry of this isomer is planar, as is the case for *t**t**t*-DPH. It is pleasing, therefore, that ΔS_{tct} is close to 0 eu. Eliel et al. proposed that the nonplanarity of *cis*-stilbene accounts for its slightly higher entropy relative to *trans*-stilbene.⁸ Nonplanarity due to the terminal *cis* double bonds may, similarly, cause the *c**t**t*- and *c**c**t*-DPH structures to explore larger ranges of torsional space

(6) The equation is based on 17 selected density values in the 0–80 °C range compiled in: Timmermans, J. *Physico-Chemical Constants of Pure Organic Compounds*; Elsevier: New York, 1950; Elsevier: New York, 1965; Vol. 2.

(7) Lunde, K.; Zechmeister, L. *J. Am. Chem. Soc.* **1954**, *76*, 2308–2313. (8) Saltiel, J.; Ganapathy, S.; Werking, C. *J. Phys. Chem.* **1987**, *91*, 2755–2758.

(9) Eliel, E. L.; Engelsman, J. J. *J. Chem. Educ.* **1996**, *73*, 903–905. (10) Ushakov, E. N.; Lednev, I. K.; Alfimov, M. V. *Dokl. Acad. Nauk. SSR* **1990**, *313*, 903.

(11) Lewis, F. D.; Yoon, B. A.; Arai, T.; Iwasaki, T.; Tokumaru, K. *J. Am. Chem. Soc.* **1995**, *117*, 3029–3036.

(12) Wharton, J. T.; Wang, S.; Saltiel, J. Unpublished results.

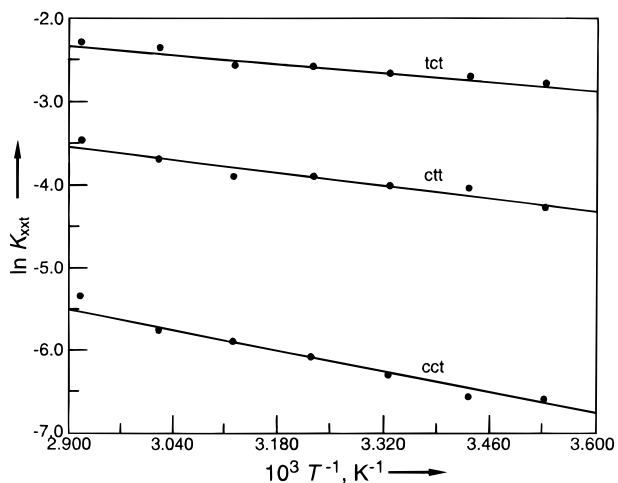


Figure 1. Thermal equilibrium constants defined in eqs 1–3 plotted according to eq 4.

Table 4. Enthalpy and Entropy Differences between Ground State *ttt*-DPH and Its Isomers^a

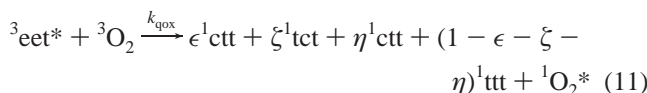
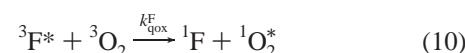
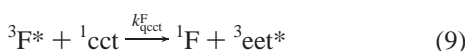
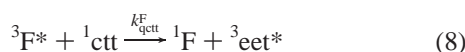
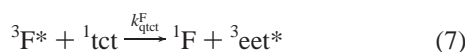
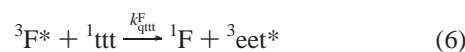
	$ttt \rightleftharpoons ctt$	$ttt \rightleftharpoons tct$	$ttt \rightleftharpoons cct$
ΔH , kcal/mol	2.24 (0.28)	1.49 (0.17)	3.95 (0.33) 3.53 (0.06) ^b
ΔS , cal/(mol K)	-0.48 (0.90)	-0.24 (0.56)	0.67 (1.06) -0.68 (0.18) ^b

^a The numbers in parentheses are from the standard deviations of the intercepts and slopes in Figure 1. ^b These values were obtained by including the point (0, -0.36) in the data set (see text).

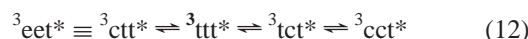
than in the planar *ttt*-DPH. However, this effect should be moderated here by the greater importance of *s-cis* conformers in *ttt*-DPH¹³ and small entropy differences were expected for these two *cis* isomers. This is consistent with the experimental ΔS_{ctt} and ΔS_{cct} values which are also within experimental uncertainty of zero. Forcing the intercept of the *cct*-DPH plot to a value of ΔS_{cct} , roughly equal to the $\Delta S_{tct} + \Delta S_{ctt}$ sum, reduces ΔH_{cct} by only 0.4 kcal/mol to 3.53 kcal/mol, Table 4.

The Triplet State. The significant differences between stilbene triplets and DPH triplets were discussed recently.³ Extended conjugation afforded by the two additional double bonds in DPH lowers the energies of planar relative to twisted triplet conformations. Equilibrium compositions favor twisted triplet geometries, ${}^3p^*$, in stilbene, but they favor planar triplet geometries in DPH.³ This geometry difference, for example, accounts for the 1000-fold longer lifetime of DPH triplets relative to stilbene triplets, despite the smaller $T_1 - S_0$ energy gap in DPH.³ In degassed benzene solution, the DPH triplet exists as an equilibrium mixture of isomeric ${}^3ttt^*$, ${}^3tct^*$, ${}^3ctt^*$, and ${}^3cct^*$ triplets, designated as ${}^3eet^*$.³ Transient observations have established that at infinite dilution at ambient temperature (20–22 °C), the lifetime of the ${}^3eet^*$ is $59.3 \pm 0.8 \mu s$.³ Self-quenching reduces the triplet lifetime to roughly $32 \mu s$ at 4×10^{-3} M *ttt*-DPH.³ Under these conditions photoisomerization occurs primarily via bimolecular quantum chain processes.³ The equilibration of isomeric DPH triplets is complete even in air-saturated solutions³ where essentially all ${}^3eet^*$ decay is via oxygen quenching and the lifetime of ${}^3eet^*$ is thereby reduced to 100 ns.^{14,15} The short lifetime eliminates quantum chain photoisomerization events and simplifies the photoisomerization

mechanism as shown below



where ${}^3eet^*$ is the equilibrating set of planar DPH triplets:



and the Greek letters in eq 11 are the effective decay fractions to each ground-state isomer. Application of the steady-state approximation on all excited species gives the following photostationary state (PSS) expressions.

$$\frac{[tct]_s}{[ttt]_s} = \left(\frac{k_{qtt}^F}{k_{qtct}^F} \right) \left(\frac{\zeta}{1 - \epsilon - \zeta - \eta} \right) \quad (13)$$

$$\frac{[ctt]_s}{[ttt]_s} = \left(\frac{k_{qtt}^F}{k_{qctt}^F} \right) \left(\frac{\epsilon}{1 - \epsilon - \zeta - \eta} \right) \quad (14)$$

$$\frac{[cct]_s}{[ttt]_s} = \left(\frac{k_{qtt}^F}{k_{qcct}^F} \right) \left(\frac{\eta}{1 - \epsilon - \zeta - \eta} \right) \quad (15)$$

These expressions require that photostationary DPH compositions be DPH concentration independent as was established in ref 3. The first factors on the right-hand side of eqs 13–15 are ratios of two highly exothermic triplet excitation transfer steps from fluorenone to each of two DPH isomers. Since such processes are known to occur at or close to the diffusion-controlled limit, the rate constant ratios should be close to unity and temperature independent. Assuming that oxygen does not differentiate between DPH triplets, eq 11 provides a snapshot of the isomeric composition of the equilibrium mixture. This means that the second factors on the right side of eqs 13–15 are the triplet equilibrium constants K_{tct}^* , K_{cct}^* , and K_{cct}^* , respectively,

$$K_{tct}^* = \frac{[{}^3tct^*]}{[{}^3ttt^*]} = \frac{\zeta}{1 - \epsilon - \zeta - \eta} \quad (16)$$

$$K_{cct}^* = \frac{[{}^3ctt^*]}{[{}^3ttt^*]} = \frac{\epsilon}{1 - \epsilon - \zeta - \eta} \quad (17)$$

$$K_{cct}^* = \frac{[{}^3cct^*]}{[{}^3ttt^*]} = \frac{\eta}{1 - \epsilon - \zeta - \eta} \quad (18)$$

The temperature dependence of the photostationary state ratios, Table 3, should therefore reveal the enthalpy differences between the isomeric triplets. The fractions ϵ and ζ can also be obtained

(13) Saltiel, J.; Sears, D. F., Jr.; Sun, Y.-P.; Choi, J.-O. *J. Am. Chem. Soc.* **1992**, *114*, 3607–3612.

(14) Görner, H. *J. Photochem.* **1982**, *19*, 343–356.

(15) Chattopadhyay, S. K.; Das, P. K.; Hug, G. L. *J. Am. Chem. Soc.* **1982**, *104*, 4507–4514.

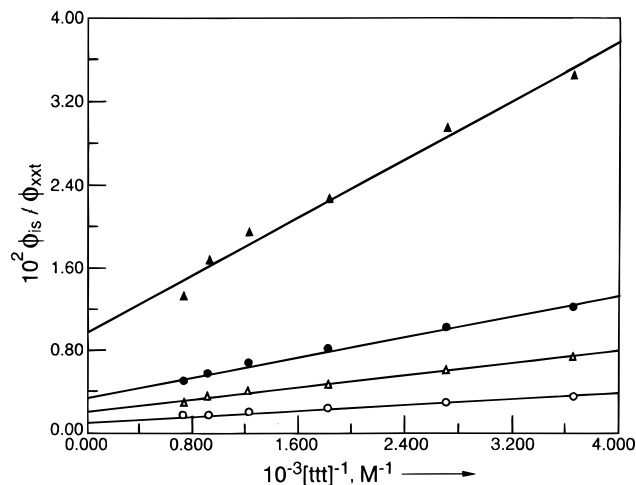


Figure 2. Plots of *tct*- (open symbols) and *ctt*-DPH (closed symbols) formation quantum yields for the fluorenone-sensitized photoisomerization of *ttt*-DPH in aerated benzene at 8.7 (Δ) and 60.0 °C (○), based on eqs 19 and 20.

Table 5. The Temperature Dependence of Equilibrium Fractions and Constants for Triplet DPH Isomers Relative to ³*ttt*-DPH^a

<i>T</i> , °C	ε	ζ	10 ² <i>K</i> _{ctt} [*]	10 ² <i>K</i> _{tct} [*]
8.7	0.0100(10)	0.0456(27)	1.06(11)	4.84(30)
20.0	0.0117(8)	0.0504(34)	1.24(10)	5.37(39)
32.2	0.0151(20)	0.0590(67)	1.63(22)	6.37(78)
45.5	0.0190(20)	0.0674(50)	2.08(24)	7.38(60)
60.0	0.0271(22)	0.0802(40)	3.03(27)	8.98(51)

^a Values in parentheses are uncertainties in the last significant figures shown.

from the *ttt*-DPH isomerization quantum yields (QY) by using the following expressions³

$$\frac{\phi_{\text{is}}}{\phi_{\text{tct}}} = \frac{1}{\zeta} \left(1 + \frac{k_{\text{qox}}^{\text{F}}[\text{O}_2]}{k_{\text{qtt}}^{\text{F}}[\text{ttt}]} \right) \quad (19)$$

$$\frac{\phi_{\text{is}}}{\phi_{\text{ctt}}} = \frac{1}{\epsilon} \left(1 + \frac{k_{\text{qox}}^{\text{F}}[\text{O}_2]}{k_{\text{qtt}}^{\text{F}}[\text{ttt}]} \right) \quad (20)$$

where ϕ_{is} is the intersystem crossing yield of fluorenone. The value of η could be obtained by use of the analogous expression for ϕ_{ctt} , but the ϕ_{ctt} values were too small to measure. Plots for the lowest and highest temperature quantum yields in Table 3, Figure 2, illustrate the adherence of the data to eqs 19 and 20. Equilibrium fractions ϵ and ζ , obtained from the inverse of the intercepts of these plots, are collected in Table 5. Also shown in Table 5 are equilibrium constants estimated from $\epsilon/(1 - \epsilon - \zeta)$ and $\zeta/(1 - \epsilon - \zeta)$, since the η values are negligibly small (see below). The adherence of these equilibrium constants to eq 4 is very good, but least-squares plots give unexpectedly high $\Delta S_{\text{ctt}}^* = 4.3 \pm 1.0$ eu and $\Delta S_{\text{tct}}^* = 2.0 \pm 0.4$ eu values. Naturally, the ΔH^* values are also high (3.8 ± 0.3 and 2.3 ± 0.1 kcal/mol for *ctt* and *tct*, respectively). As pointed out for the ground-state isomers, the entropy differences are expected to be close to zero, consequently, as an alternative treatment, the intercepts of these plots were forced to be nearly zero, Figure 3. Thermodynamic quantities with and without the $\Delta S^* = 0$ assumption are shown in Table 6. The plots in Figure 3 were used to calculate K_{ctt}^* and K_{tct}^* values at the temperatures in Table 2. As expected, the ratio of the equilibrium constants to the photostationary state ratios in Table 2 give excitation transfer

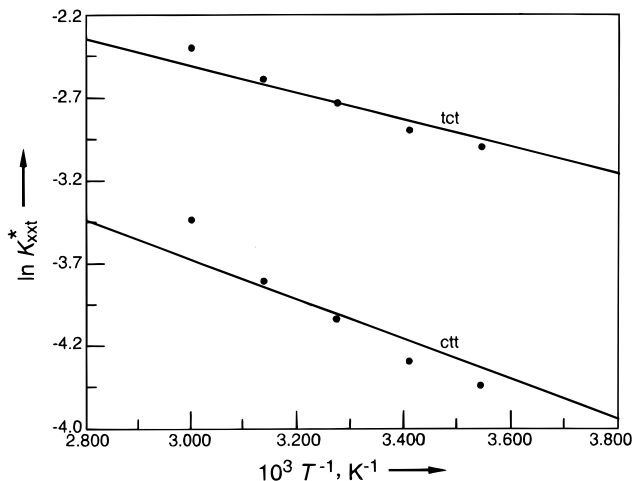


Figure 3. Triplet equilibrium constants defined in eqs 16 and 17 plotted according to eq 4; plots forced to zero intercepts (see text).

Table 6. Enthalpy Differences between Triplet State *ttt*-DPH and Its Isomers^a

	³ <i>ttt</i> * ⇌ ³ <i>ctt</i> *	³ <i>ttt</i> * ⇌ ³ <i>tct</i> *	³ <i>ttt</i> * ⇌ ³ <i>cct</i> *
	ΔH^* , kcal/mol		
QY	3.80(31)	2.27(12)	
	2.51(10) ^b	1.68(5) ^b	
PSS	2.92(12)	1.49(8)	5.52(28)
	2.49(4) ^b	1.66(3) ^b	4.11(11) ^b
	ΔS^* , eu		
QY	4.33(100)	1.96(39)	
	0.07(30) ^b	0.03(13) ^b	
PSS	1.40(40)	-0.62(26)	4.53(90)
	0.00(12) ^b	0.00(10) ^b	0.00(36) ^b

^a Values shown in parentheses are uncertainties (standard deviations) in the last significant figures shown. ^b Intercepts fixed to $\Delta S^* \approx 0$.

rate constant ratios ($k_{\text{qctt}}^{\text{F}}/k_{\text{qtt}}^{\text{F}} = 1.09 \pm 0.05$ and ($k_{\text{qctt}}^{\text{F}}/k_{\text{qtt}}^{\text{F}} = 1.33 \pm 0.05$ that are close to unity and, within experimental uncertainty, temperature independent. This rate constant order for excitation transfer from fluorenone triplets to the DPH isomers is the same as predicted earlier on the basis of results at one temperature,³ but spans a somewhat narrower range: $k_{\text{qtt}}^{\text{F}}:k_{\text{qctt}}^{\text{F}}:k_{\text{qtct}}^{\text{F}} = 1.00:1.09:1.33$.

The relationship of the $[\text{tct}]_s/[\text{ttt}]_s$ ratio to temperature is given by

$$\ln \left(\frac{[\text{tct}]_s}{[\text{ttt}]_s} \right) = -\frac{\Delta H_{\text{tct}}^*}{RT} + \frac{\Delta S_{\text{tct}}^*}{R} + \ln \frac{k_{\text{qtt}}^{\text{F}}}{k_{\text{qctt}}^{\text{F}}} \quad (21)$$

and analogous expressions can be written for the $[\text{ctt}]_s/[\text{ttt}]_s$ and $[\text{cct}]_s/[\text{ttt}]_s$ ratios. Thermodynamic quantities from these plots are also shown in Table 6. Since no estimate of the $k_{\text{qtt}}^{\text{F}}/k_{\text{qctt}}^{\text{F}}$ ratio is available, it was assumed equal to $(k_{\text{qtt}}^{\text{F}})^2/(k_{\text{qctt}}^{\text{F}}k_{\text{qtct}}^{\text{F}})$. The more precise PSS data give ΔS^* values for *tct* and *ctt* that are much closer to zero than the values obtained from the QY data. Again as an alternative treatment, the plots in Figure 4 were forced to zero intercepts, and the resulting ΔH^* values are shown in Table 6. It can now be seen that when the $\Delta S^* \approx 0$ condition is uniformly imposed, the enthalpy differences obtained independently from the quantum yields and from the photostationary states are in excellent agreement. As in the case of the ground-state enthalpy differences the relationship $\Delta H_{\text{ctt}}^* + \Delta H_{\text{tct}}^* = \Delta H_{\text{cct}}^*$ is adhered to remarkably well. Furthermore, the enthalpy differences between the DPH isomers in the ground and triplet states are nearly identical.*

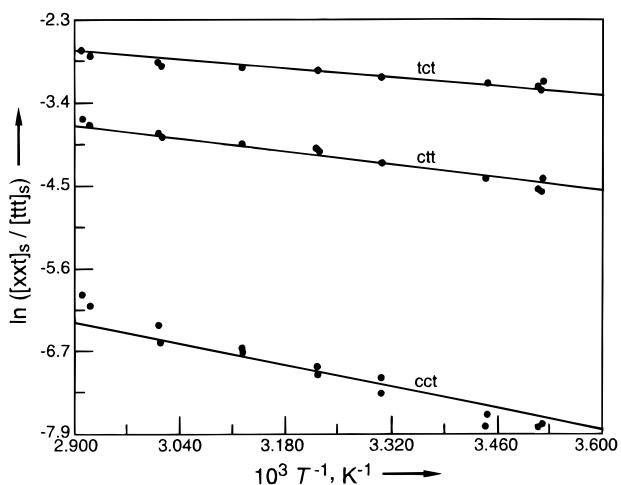


Figure 4. Photostationary ratios plotted according to eq 21 and forced to $\Delta S^* = 0$ intercepts (see text).

The Biradicals. The relaxed geometries of the triplet states of the stilbenes,^{8,16,17} 1,3-dienes,^{16–18} and related simple alkenes, generally, correspond to twisted species with orthogonal 2p orbitals at the relaxation site. They are close in energy and geometry to the biradical transition states for thermal cis–trans isomerization.^{8,17,19} The proximity between S_0 and T_1 surfaces at these relaxed geometries leads to rapid $T_1 \rightarrow S_0$ decays and short triplet lifetimes in the nanosecond time scale. DPH triplets, on the other hand, have global energy minima at planar geometries. Decay from these geometries is subject to substantial $S_0 - T_1$ energy gaps leading to a 10^3 -fold longer triplet lifetime.³ The enthalpy differences determined in this work together with the known 34.0 kcal/mol energy^{15,20–22} of ${}^3\text{ttt-DPH}^*$ locate the relative energies of the *ttt*, *ctt*, *tct*, and *cct* isomers on the ground and triplet energy surfaces. Complete equilibration³ of the isomeric DPH triplets within the 100 ns triplet lifetime in air-saturated benzene^{14,15} requires interconversion rate constants greater than 10^8 s^{-1} . Assuming a normal preexponential factor of 10^{13} s^{-1} for these adiabatic unimolecular processes requires that activation energies for the interconversions be no larger than 6.9 kcal/mol. This corresponds to a limiting activation enthalpy of 6.3 kcal/mol at 20 °C and places twisted triplets at energies no higher than 40.3 kcal/mol relative to the ground state of *ttt-DPH*.

Since activation enthalpies for *tct* \rightarrow *tt* and *ctt* \rightarrow *ttt* isomerizations are not available for DPH, the energies of the singlet biradicals corresponding to the transition states of these reactions are unknown. The energy of the symmetrical orthogonal biradical derived by a 90° twist about the central double bond of *ttt-DPH* can be estimated by reversing, in part, the procedure used by Doering and co-workers. In an elegant series

(16) Hammond, G. S.; Saltiel, J.; Lamola, A. A.; Turro, N. J.; Bradshaw, J. S.; Cowan, D. O.; Vogt, V.; Dalton, C. *J. Am. Chem. Soc.* **1964**, *86*, 3197–3217.

(17) Ni, T.; Caldwell, R. A.; Melton, L. A. *J. Am. Chem. Soc.* **1989**, *111*, 457–464.

(18) Saltiel, J.; Rousseau, A. D.; Sykes, A. *J. Am. Chem. Soc.* **1972**, *94*, 5903–5905.

(19) Unett, D. J.; Caldwell, R. A. *Res. Chem. Intermed.* **1995**, *21*, 665–709.

(20) Heinrich, G.; Holzer, G.; Blume, H.; Schulte-Frohlinde, D. Z. *Naturforsch.* **1970**, *25b*, 496.

(21) Evans, D. F.; Tucker, J. N. *J. Chem. Soc., Faraday Trans. 2* **1972**, *68*, 174.

(22) (a) Ramamurthy, V.; Caspar, J. V.; Corbin, D. R.; Schyler, B. D.; Maki, A. H. *J. Phys. Chem.* **1990**, *94*, 3191–3193. (b) Ramamurthy, V.; Caspar, J. V.; Eaton, D. F.; Kuo, E. W.; Corbin, D. R. *J. Am. Chem. Soc.* **1992**, *114*, 3882–3892.

of papers,²³ they measured activation enthalpies for the thermal isomerization of several related polyenes. These activation enthalpies were used to evaluate the effect of additional conjugated double bonds on the enthalpies of stabilization, SE_n , of polyenyl radicals of type $\text{H}(\text{CH}=\text{CH})_n\dot{\text{C}}\text{H}_2$. The relative energies of the coplanar polyenes were obtained by applying an additive constant $K = 3.74 \text{ kcal/mol}$, the Kistiakowski unit,^{23a} for each conjugative interaction between successive double bonds. Theory, at all levels employed thus far,^{24–26} predicts the linear relationship between the enthalpy of conjugation and the order of the polyene, but the value of K is empirically derived^{23a} from thermochemical data on butadiene²⁷ and methyl derivatives²⁸ and on hexa-1,3,5-triene.²⁹ Starting with an allyl stabilization enthalpy, $SE_1 = 13.5 \text{ kcal/mol}$,³⁰ the increase in stabilization was found to diminish with each successive double bond.²³ Namely, SE_2 , SE_3 , and SE_4 are 16.9, 19.2, and 20.7 kcal/mol, respectively, such that even the first increment, $SE_2 - SE_1$, is a little smaller than K .

The enthalpy of conjugation for a phenyl–vinyl coplanar interaction, $K' = 3.5 \text{ kcal/mol}$, has been based on the difference between the heats of hydrogenation of *trans*-2-butene and *trans*-stilbene.^{31,32} This value is close to the barrier ($\sim 3.3 \text{ kcal/mol}$) calculated for the torsion of the phenyl group in *trans*-stilbene at the ab initio 3-21G level of theory.³³ Provided that K and K' units be additive, conjugative stabilization energies of the coplanar *all-trans*- α,ω -diphenylpolyenes, $\text{Ph}(\text{CH}=\text{CH})_n\text{Ph}$, should be given by $2K' + (n - 1)K$. Experimental validation of this relationship rests on the stabilization energy of 1,4-diphenyl-1,3-butadiene, 10.7 kcal/mol,³¹ which coincides with $2K' + K = 10.74 \text{ kcal/mol}$. We therefore take 14.5 kcal/mol as the conjugative stabilization energy of *ttt*-DPH. The relative energies of the biradical transition states for cis–trans isomerization about a specific bond could be estimated if the stabilization energies of the resulting pairs of radical moieties were known. The conjugative stabilization energies of the benzyl, SE_{Bz} , and of the 1-phenylallyl, SE_{PhA} , radicals are required to estimate ground-state biradical energies for stilbene, 1,4-diphenyl-1,3-butadiene, and for central bond rotation in *ttt*-DPH. Recommended CH bond energies³⁴ for ethane and toluene give $SE_{Bz} = 12.6 \text{ kcal/mol}$ for the benzyl radical, but there is no empirical SE_{PhA} value for the 1-phenylallyl radical. Figure 5 shows a plot

(23) (a) Doering, W. von E.; Kitagawa, T. *J. Am. Chem. Soc.* **1991**, *113*, 4288–4297. (b) Doering, W. von E.; Birladeanu, L.; Cheng, X.-h.; Kitagawa, T.; Sarma, K. *J. Am. Chem. Soc.* **1991**, *113*, 4558–4563. (c) Doering, W. von E.; Sarma, K. *J. Am. Chem. Soc.* **1992**, *114*, 6037–6043. (d) Doering, W. von E.; Shi, Y.-q.; Zhao, D.-c. *J. Am. Chem. Soc.* **1992**, *114*, 10763–10766.

(24) Heilbronner, E.; Bock, H. *Das HMO-Modell und seine Anwendung*; Verlag Chemie: Weinheim, 1970; Vol. 3, pp 16–42.

(25) (a) Dewar, M. J. S.; Gleicher, G. J. *J. Am. Chem. Soc.* **1965**, *87*, 685–692. (b) Dewar, M. J. S.; de Liano, C. *J. Am. Chem. Soc.* **1969**, *91*, 789–802.

(26) (a) Hess, B. A., Jr.; Schaad, L. V. *Pure Appl. Chem.* **1980**, *52*, 1471–1494. (b) Hess, B. A., Jr.; Schaad, L. J. *J. Am. Chem. Soc.* **1983**, *105*, 7500–7505.

(27) Kistiakowsky, G. B.; Ruhoff, J. R.; Smith, H. A.; Vaughan, W. E. *J. Am. Chem. Soc.* **1936**, *58*, 146–153.

(28) Pedley, J. B.; Naylor, R. D.; Kirby, S. P. *Thermochemical Data of Organic Compounds*, 2nd ed.; Chapman and Hall: London, 1986.

(29) Turner, R. B.; Mallon, B. H.; Tichy, M.; Doering, W. von E.; Roth, W. R.; Schröder, G. *J. Am. Chem. Soc.* **1973**, *95*, 8605–8610.

(30) Doering, W. von E.; Roth, W. R.; Bauer, F.; Boenke, M.; Breuckmann, R.; Ruhkamp, J.; Wortmann, O. *Chem. Ber.* **1991**, *124*, 1461–1470.

(31) Williams, R. B. *J. Am. Chem. Soc.* **1942**, *64*, 1395–1404.

(32) Wheland, G. W. *Resonance in Organic Chemistry*; Wiley: New York, 1955; p 80.

(33) Lhost, O.; Brédas, J. L. *J. Chem. Phys.* **1992**, *96*, 5279–5288.

(34) Berkowitz, J.; Ellison, G. B.; Gutman, D. *J. Phys. Chem.* **1994**, *98*, 2744–2765.

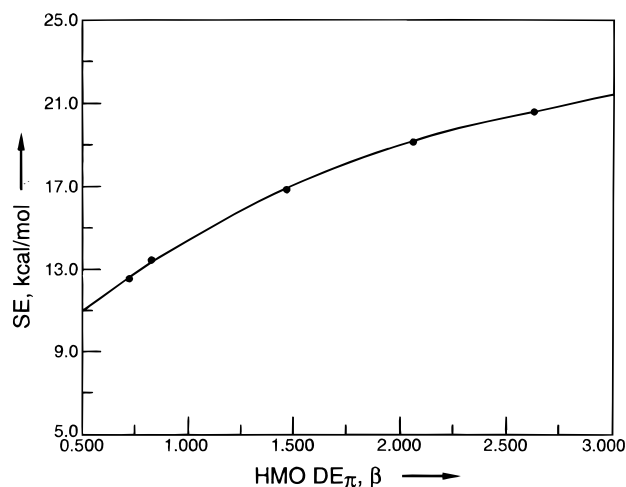


Figure 5. Experimental stabilization energies for the polyenyl^{22c} and benzyl radicals plotted against Hückel MO π -delocalization energies.

of SE_n values for the polyenyl radicals^{23c} ($n = 1-4$) against the corresponding HMO DE_π values.³⁵ The dependence of SE_n on DE_π is far from linear, but it is monotonic. Furthermore, the point for the benzyl radical ($DE_\pi = 0.72\beta$) falls nicely on the same curve. A polynomial fit of all five points gives $SE_{PhA} = 16.6$ kcal/mol as an estimate of the stabilization energy of the 1-phenylallyl radical ($DE_\pi = 1.38\beta$). Interestingly, this value is nearly identical with the average of $SE_1 + K' = 17.0$ kcal/mol and $SE_{Bz} + K = 16.3$ kcal/mol. The biradical obtained by rotation about one of the terminal double bonds in DPH consists of benzyl and 1-phenylpentadienyl moieties. The stabilization energy of the latter, SE_{PhP} , is not known but, based on HMO $DE_\pi = 1.98\beta$, Figure 5 gives $SE_{PhP} = 18.9$ kcal/mol, sensibly close to the value for the heptatrienyl radical.^{23c}

The predicted enthalpies of activation for the α,ω -diphenylpolyenes, $n = 1-3$, are derived as shown in Scheme 1. Following Doering and co-workers, we use 65.9 ± 0.9 kcal/mol as the activation enthalpy for the model monoolefin, neglecting steric effects in the planar ground states and in the biradicals.^{23a,36} Applying the stabilization energies for the radical moieties and for the coplanar ground-state molecules gives $\Delta H^\ddagger = 47.2, 43.9$ and 40.2 kcal/mol as the transition state enthalpies of stilbene, 1,4-diphenyl-1,3-butadiene, DPB, and central bond DPH isomerization, respectively. The enthalpy of activation for terminal bond isomerization in DPH is not shown in Scheme 1. Our estimated value, 41.6 kcal/mol, is a little higher than the activation enthalpy for central bond isomerization. The value for stilbene agrees well with experimental measurements of this quantity that place it at 47.4 ± 1.6 kcal/mol,^{8,9,37-39} and with a calculated value of 48.9 kcal/mol based on Benson equivalents.¹⁷ No experimental values are available for DPB and DPH, but the prediction that isomerization activation enthalpies decrease progressively as one moves from stilbene to the two higher vinylogues is reasonable.

We concluded above that the energies of the triplet biradicals of DPH can be no higher than 40.3 kcal/mol. The estimated

Scheme 1

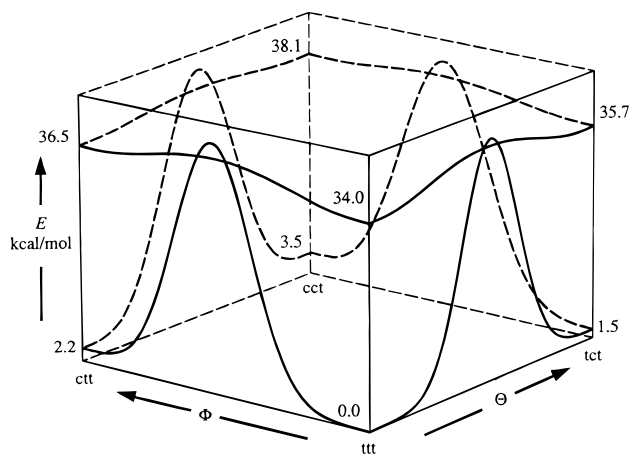
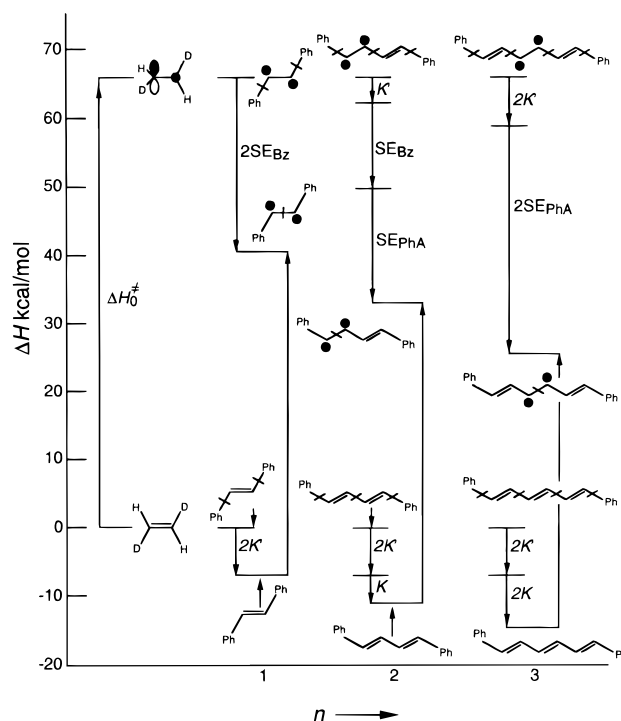


Figure 6. Ground state and triplet potential energy curves for twisting about C_1C_2 (ϕ) and C_3C_4 (θ) in DPH.

value for the symmetrical singlet biradical is nearly identical with that limit, but that for the unsymmetrical biradical is 1.3 kcal/mol higher. In view of the uncertainty in these values, the question of whether singlet and triplet potential energy surfaces are separated by a small energy gap, touch, or cross close to the biradical DPH geometries remains open. However, S_0 and T_1 surfaces are more likely to cross upon terminal bond rotation. Since the 40.3 kcal/mol value is an upper limit, the potential energy curves in Figure 6 are tentatively shown to cross. Earlier, one of us had come to the conclusion that S_0 and T_1 surfaces cross in the case of the stilbenes.⁸ Since then, time-resolved photoacoustic calorimetry measurements have placed ${}^3p^*$, the stilbene triplet biradical, at 46.5 ± 0.9 kcal/mol,¹⁷ somewhat below, but well within experimental uncertainty of the energy of the singlet biradical. The categorical nature of the prediction that $S_0 - T_1$ surface crossing is required in stilbene was therefore rightly questioned.^{17,40}

Conclusion

Figure 6 gives a pictorial representation of our results.

(35) Streitwieser, A., Jr. *Molecular Orbital Theory for Organic Chemists*, Wiley: New York, 1961; pp 46, 393, and 396.

(36) Doering, W. von E.; Roth, W. R.; Bauer, F.; Breuckmann, R.; Ebrecht, T.; Herbold, M.; Schmidt, R.; Lennartz, H.-W.; Lenoir, D.; Boese, R. *Chem. Ber.* **1989**, *122*, 1263-1275.

(37) Kistiakowsky, G. B.; Smith, W. R. *J. Am. Chem. Soc.* **1934**, *56*, 638.

(38) Santoro, A. V.; Barrett, E. J.; Hoyer, H. H. *J. Am. Chem. Soc.* **1967**, *89*, 4545-4546.

(39) Schmiegel, W. W.; Litt, F. A.; Cowan, D. O. *J. Org. Chem.* **1968**, *33*, 3334.

Placement of the global energy minimum of the DPH triplet state at the all-trans geometry is consistent with early observations that led Görner¹⁴ and Das et al.¹⁵ to assign the all-trans geometry to the DPH triplet. However, the energetic landscape of Figure 6 allows the presence of significant populations of planar triplet geometries containing cis double bonds. The depiction of twisted triplet geometries as torsional transition states for the interconversion of DPH triplets is consistent with our calculated triplet biradical energies. Figure 6 reverses the energetics of twisted vs planar geometries that apply to the prototypical stilbene triplets, and the 10³-fold increase of the DPH triplet lifetime relative to that of stilbene is a direct consequence of this maximum/minimum reversal.^{3,14,15}

The relationship of the triplet energy of each of the isomeric DPH triplets, E_T^{xxt} where x is either t or c, to the triplet energy of *ttt*-DPH is given by

$$E_T^{xxt} = E_T^{ttt} + \Delta H_{xxt}^* - \Delta H_{xxt} \quad (22)$$

With reference to $E_T^{ttt} = 34.0$ kcal/mol,^{15,20–22} the triplet energies of the cis isomers are 34.3 ± 0.3 , 34.2 ± 0.2 , 34.6 ± 0.4 kcal/mol and for *ctt*-, *tct*-, and *cct*-DPH, respectively. The prediction of nearly identical triplet energies for the isomeric triplets is nicely consistent with the interpretation of fluorenone-sensitized photoisomerization quantum yields under degassed conditions.³ These quantum yields are dominated by quantum chain processes involving triplet excitation transfer between the DPH isomers. Rate constants in benzene for excitation transfer steps in both directions between the *ttt*, *tct*, and *ctt* isomers cluster in the narrow range of $(2.1–3.6) \times 10^8$ M⁻¹ s⁻¹ revealing no energetic advantage for transfer in a specific direction.³ On the basis of Figure 6, the 25- to 40-fold deviation of these rate constants from the nearly diffusion controlled value expected for isoenergetic triplet excitation transfer may seem surprising.³ Energy minima at planar geometries in T₁ and S₀ surfaces require that triplet excitation transfer between the DPH isomers be vertical with respect to torsional coordinates. The seeming contradiction arises because Figure 6 does not reveal geometry changes, reflecting the reversal of the order of alternating double/single bonds in the triene moiety that accompanies S₀ → T₁

(40) The maximum triplet energy of ³p* was erroneously estimated in ref 8 as ~44 kcal/mol. Actually, the maximum value given by the sum of the triplet energy of 9,10-dichloroanthracene, DCA, and the activation enthalpy for triplet excitation transfer from DCA to *trans*-stilbene, 45.5 ± 0.5 kcal/mol,⁴⁰ is in good agreement with the calorimetric value.

excitation. The noninterconverting ground-state DPH isomers become rapidly equilibrating conformers in the triplet state. Triplet excitation transfer events between DPH isomers are nonvertical with respect to CC stretching vibrational modes,³ and this is probably the major source of their inefficiency. In the stilbenes, where the major geometry change on S₀ → T₁ excitation is along the torsional coordinate, descriptions of nonvertical triplet excitation transfer have focused naturally on Franck–Condon (FC) factors involving torsional modes. However, CC bond length changes are similarly expected in the stilbenes, and it is likely that unfavorable FC overlap factors involving CC stretching modes also contribute to the determination of the overall efficiency of nonvertical triplet excitation in the prototypical stilbene system.

We conclude that a general requirement for the participation of quantum chain events in triplet state olefin photoisomerization is a rather flat triplet potential energy surface with shallow minima or maxima at twisted geometries. In either case, planar geometries must be energetically accessible so that sufficiently large S₀ – T₁ energy gaps are attained to permit the olefin triplet to function as a donor. Conjugated alkadienes, for which quantum chain photoisomerization was first demonstrated,⁴² having global energy minima at twisted geometries are at one extreme. Their short triplet lifetimes, in the nanosecond time scale, require large concentrations for the quantum chain process to contribute in photoisomerization. The diphenylhexatrienes and styrylarenes with polybenzenoid aromatic rings, of which the 2-styrylanthracenes provide the most prominent example,² are at the other extreme. For such molecules, energy minima at planar geometries on the triplet potential energy surface ensure much longer triplet lifetimes and allow efficient participation of the quantum chain process at much lower concentrations.

Theoretical calculations of the energetics for *trans* ⇌ *cis* isomerization in S₀ and T₁ DPH are not available. Figure 6 should provide a stimulus and an empirical test for such calculations in the future.

Acknowledgment. This research was supported by NSF, most recently, by Grant CHE-9612316. J.S. dedicates this paper to the memory of the late Professor R. B. Turner who showed the way to Caltech.

JA982551J

(41) Saltiel, J.; Marchand, G. R.; Kirkor-Kaminska, E.; Smothers, W. K.; Mueller, W. B.; Charlton, J. L. *J. Am. Chem. Soc.* **1984**, *106*, 3144–3151.

(42) Saltiel, J.; Townsend, D. E.; Sykes, A. *J. Am. Chem. Soc.* **1973**, *95*, 5968–5973.